Functional nanocomposites based on the infusion or *in situ* generation of nanoparticles into amphiphilic epoxy gels

Ana Ledo-Suárez,[ab] Julieta Puig,[a] Ileana A. Zucchi,[a] Cristina E. Hoppe,*[a] María L. Gómez,[a] Roberto Zysler,[c] Carlos Ramos,[c] M. Claudia Marchi,[d] Sara A. Bilmes,[d] Massimo Lazzari,[b] M. Arturo López-Quintela[b] and Roberto J. J. Williams*[a]

Received 12th May 2010, Accepted 8th September 2010
DOI: 10.1039/c0jm01421d

The production of nanocomposites with functional properties *via* the infusion of preformed nanoparticles (NPs) or their *in situ* generation inside an amphiphilic epoxy gel is reported. The gel was synthesized by the reaction of a diepoxy monomer based on diglycidyl ether of bisphenol A with an *n*-alkylamine, followed by annealing the resulting linear polymers above their glass transition temperatures to produce physical gelation through tail-to-tail association of pendant alkyl chains. Some of the advantages of these polymer gels are: (a) they have a low crosslink density and can therefore be significantly swollen by several organic solvents, (b) the presence of pendant alkyl chains provides a convenient chemical environment for the stabilization of NPs coated with alkyl chains, (c) the presence of secondary hydroxyls and tertiary amine groups in the polar backbone of polymer chains can be used to coordinate and reduce different precursors of NPs. Preformed NPs could be successfully infused into the gels keeping their optical properties (*e.g.*, CdSe quantum dots) or magnetic behavior (*e.g.*, γ-Fe_2O_3@oleic acid NPs) in the resulting nanocomposite. *In situ* generation of Au and Ag NPs (average size close to 10 nm) inside the amphiphilic gels was produced by infusing $HAuCl_4$ or $AgNO_3$ followed by reduction to the corresponding metals with secondary alcohols present in the polymer backbone, at 100 °C. Amphiphilic gels were employed as hosts for the *in situ* precipitation of gold(I)-dodecanethiolate leading to films exhibiting a red emission (638 nm) when excited with UV light (300 nm).

Introduction

The synthesis and characterization of a large variety of nanoparticles (NPs) stabilized with organic ligands and with potential uses derived from their functional properties (optical, magnetic, sensorial, *etc.*) have been the subject of many publications in recent years.[1–9] In order to build up functional materials, devices or actuators based on these NPs they have to be embedded or supported into or over a specific host. Due to their high versatility, polymers are usually selected for these purposes.[10–15] There are different strategies for dispersing NPs into a polymeric matrix.[10,11,13–15] One possibility is to start from a homogeneous dispersion of the NPs into the polymer precursors (mixture of monomers, co-monomers, catalysts or initiators, *etc.*), and produce the polymer by heating, UV-irradiation or other means. In this process, a polymerization-induced phase separation (PIPS) usually takes place, mainly due to the decrease of the entropic contribution to the free energy of mixing.[16,17] Instead of generating a uniform dispersion of individual NPs in the polymer matrix, a segregation of NPs takes place that can be used to generate useful structures and material properties. For example, the phase separation of polyhedral oligomeric silsesquioxanes (POSS) during formation of an epoxy network leads to the formation of micrometric crystalline POSS domains dispersed in the matrix, enhancing some mechanical properties of the crosslinked epoxy.[18] The occurrence of PIPS in a solution of gold NPs stabilized by dodecanethiol chains in precursors of an epoxy network led to the segregation, coalescence and self-assembly of gold NPs generating hexagonal closed-pack colloidal crystals that formed fractal structures at the air–polymer interface.[19] Polymerization of nanorods (NRs) dispersed in a monomer using UV-irradiation through a mask resulted in the segregation of the NRs from the areas rich in polymer to the areas rich in monomer. This produced the simultaneous patterning and alignment of the NRs in the polymer film.[20] PIPS in a blend of polymer precursors, a solvent and gold NRs led to a macroporous polymer where gold NRs were segregated to the surface of the pores due to the Pickering effect.[21]

When a uniform dispersion of NPs in the polymer matrix is desired other alternatives must be proposed to avoid the occurrence of PIPS. One of such alternatives is to functionalize the NPs with ligands bearing reactive groups that can participate in the polymerization reaction. In this way, the individual NPs act as crosslinking units of the polymer network. POSS bearing

[a]*Institute of Materials Science and Technology (INTEMA), University of Mar del Plata and National Research Council (CONICET), J. B. Justo 4302, 7600 Mar del Plata, Argentina. E-mail: hoppe@fi.mdp.edu.ar; williams@fi.mdp.edu.ar; Fax: +54 223 4810046; Tel: +54 223 4816600*
[b]*Departamento de Química Física, Facultad de Química, Universidad de Santiago de Compostela (USC), Campus Universitario Sur, 15782 Santiago de Compostela, España. E-mail: malopez.quintela@ucs.es; Fax: +34 981 595012; Tel: + 34 981 563100*
[c]*Centro Atómico Bariloche (CAB)—Instituto Balseiro, Av. Bustillo 9500, 8400 San Carlos de Bariloche (RN), Argentina. E-mail: zysler@cab.cnea.gov.ar; Fax: +54 2944 445102; Tel: +54 2944 445162*
[d]*Instituto de Química Física de los Materiales, Medio Ambiente y Energía(INQUIMAE) Facultad de Ciencias Exactas y Naturales, Universidad de Buenos Aires-CONICET, Ciudad Universitaria, Pabellón II, C1428EHA Buenos Aires, Argentina. E-mail: sarabil@qi.fcen.uba.ar; Fax: +54 11 4576 3341; Tel: +54 11 4576 3358*

reactive groups in the organic branches behave in this way.[22–24] Silver NPs coated with OH-functionalized organic ligands could be uniformly dispersed into an epoxy network by covalent bonds produced during the homopolymerization of the epoxy monomer.[25] Quantum dots (CdSe/ZnS NPs) could be uniformly dispersed in a cellulose hydrogel during crosslinking in a NaOH/urea aqueous system, by strong interactions of NPs and cellulose after the hydrolysis of the ligands stabilizing the NPs.[26]

Another strategy to produce a uniform dispersion of NPs in polymer matrices is to infuse or *in situ* generate the NPs into a preformed polymer gel. For example, hybrid ferrogels were synthesized infiltrating a crosslinked poly(ethylene oxide)/polysiloxane matrix with iron ions and forming nanocrystalline oxide particles by precipitation with aqueous ammonia.[27] CdSe/CdS NPs with exchanged ligands to provide water solubility were immobilized on poly(*N*-isopropylacrylamide)-based microspheres.[28] NPs were mostly attached to the surface of the beads and partially infused inside the polymer network. As shown by the last example, this strategy has significant limitations to produce uniform dispersions inside the polymers. Polymer hosts or ligands stabilizing the NPs have to be carefully selected to produce a uniform infusion of the preformed NPs or their precursors. In this manuscript we show that an amphiphilic epoxy gel, obtained by reaction of diglycidyl ether of bisphenol A (DGEBA) and an alkylamine (Fig. 1),[29] is a versatile polymer host to produce nanocomposites with a uniform distribution of NPs. Some of the advantages of these polymer gels are: (a) they have a low crosslink density produced by tail-to-tail association of alkyl chains (physical gel) and can therefore be significantly swollen by several organic solvents, (b) the presence of pendant alkyl chains provides a convenient chemical environment for the stabilization of NPs coated with alkyl chains, (c) the presence of secondary hydroxyls and tertiary amine groups in the polar backbone of polymer chains can be used to coordinate and reduce different precursors of NPs. We provide several examples where these amphiphilic polymer gels were used to generate nanocomposites with luminescent or magnetic properties.

Experimental

Materials

The diepoxy monomer was based on diglycidyl ether of bisphenol A (DGEBA, DER 332, Aldrich), with a mass per mole of epoxy groups equal to 174.3 g mol^{-1} ($n = 0.03$ in the chemical structure shown in Fig. 1). The alkylamines were dodecylamine (DA, 98 wt%, Fluka, melting temperature in the range 27–29 °C) and hexadecylamine (HA, 98 wt% Aldrich, melting temperature in the range 43–46 °C). The following chemical products (Aldrich) were used as received: dodecanethiol, hydrogen tetrachloroaurate(III) trihydrate ($HAuCl_4 \cdot 3H_2O$, ≥49 wt% as Au), tetraoctylammonium bromide, sodium borohydride, ferric chloride ($FeCl_3 \cdot 6H_2O$), ferrous sulfate ($FeSO_4 \cdot 7H_2O$), polyoxyethylen-10-oleyl ether (Brij 97), oleylamine, oleic acid, 1-octadecene, selenium powder, trioctylphosphine and cadmium oxide. Silver nitrate (Cicarelli) and different solvents were P.A. grade.

Synthesis of the amphiphilic epoxy gel

Stoichiometric amounts of DGEBA and the corresponding *n*-alkylamine were mixed by vigorous stirring at approximately

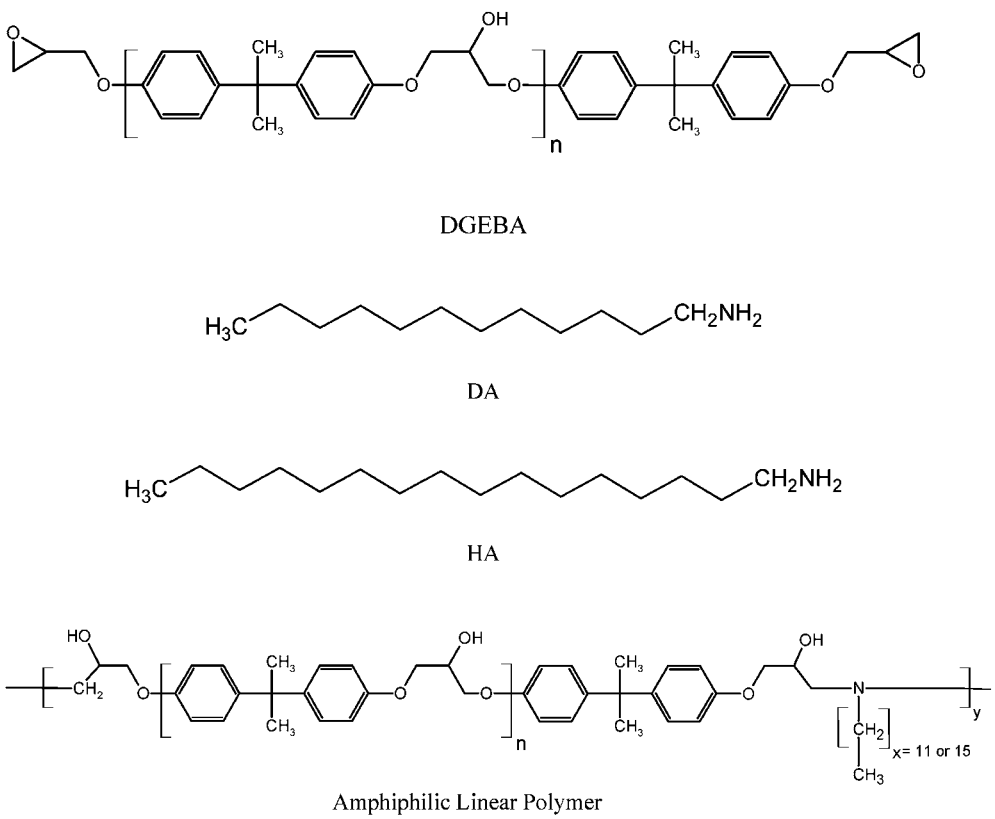

Fig. 1 Chemical structures of diglycidyl ether of bisphenol A (DGEBA), *n*-alkylamines and the amphiphilic linear polymer.

100 °C. The polymerization was carried out in bulk at 100 °C for 3 h. The reaction product was annealed at 60 °C for 21 h.

Synthesis of NPs

Gold NPs with an average size of 2 nm and coated with dodecyl chains were obtained by the Brust–Schiffrin method.[30] Briefly, 1.1 mmol of $HAuCl_4 \cdot 3H_2O$ was dissolved in a solution of tetraoctylammonium bromide in toluene. After stirring overnight, dodecanethiol (DDT) was added in a molar ratio of 0.9 with respect to gold. An excess of freshly prepared sodium borohydride aqueous solution was then added as a reducing agent. The as-synthesized DDT-coated gold NPs were separated from unattached DDT by precipitation with ethanol (in a volume ratio with respect to toluene solution of 7 : 1), followed by centrifugation (8000 rpm). The wet product was dried at 40 °C and stored as a waxy solid at room temperature.

A ferrofluid of oleic acid-capped maghemite (γ-Fe_2O_3) NPs, with a mean size of about 3 nm, was synthesized by a microemulsion method.[31] Briefly, a (cyclohexane/Brij 97/aqueous phase) system was used with an aqueous phase formed by a 2 : 1 ferric–ferrous solution. To form the NPs, oleylamine was added to the microemulsion with magnetic stirring. Final stabilization was attained by adding a 50 : 50 molar mixture of oleic acid and oleylamine on the reaction media. The obtained oleic acid-coated NPs were separated, washed and finally dispersed in tetrahydrofuran (THF) to form a stable ferrofluid.

Synthesis of CdSe quantum dots (QDs)

CdSe quantum dot nanocrystals with an average size of 3 nm were synthesized by a modification of the Murray's procedure[32] which employs less drastic and toxic conditions.[33] Briefly, a solution of Se precursor was prepared in a fume hood by combining 30 mg of Se and 5 ml of 1-octadecene in a 10 ml round-bottom flask. After adding 0.4 ml of trioctylphosphine (TOP), the solution was vigorously stirred until it turned colorless; meaning that all Se was dissolved. The round flask containing the Se precursor was sealed with a septum. The Cd precursor was prepared by adding 39 mg of CdO to a mixture of 1.8 ml of oleic acid and 30 ml of octadecene in a 50 ml round-bottom flask. The resulting mixture was subsequently heated up to ~150 °C until all Cd was dissolved (as noticed by the colorless solution). 5.3 ml of this solution were transferred into a 10 ml round-bottom flask and heated up to ~200 °C. At this point, 0.5 ml of the Se precursor was added under vigorous stirring. The synthesis was stopped after 30 s of the Se precursor addition.

Infusion of NPs into the epoxy gels

Au@DDT and γ-Fe_2O_3@oleic acid were dispersed in THF in a concentration close to 3 mg ml^{-1}. CdSe quantum dots (QDs) were dispersed in 1-octadecene/THF (50 : 50) in a concentration close to 0.3 mg ml^{-1}. Squared slices of the gel (approximately 170 mg) were immersed in 10 ml of solvent/NP dispersions for 24 h at room temperature. After this time, samples developed the characteristic color of the NPs indicating successful migration to the gel. Samples were then rinsed in THF three times and dried under vacuum at room temperature.

In situ generation of NPs and gold thiolate inside the epoxy gels

Gold and silver NPs were generated inside the gels starting from 6 mM THF or THF/H_2O (90 : 10) solutions of $HAuCl_4 \cdot 3H_2O$ and $AgNO_3$, respectively. Squared slices of the gel (approximately 170 mg) were immersed in 10 ml of the corresponding solutions for 72 h at room temperature. Then, samples were rinsed in THF three times and dried in vacuum at room temperature. Gold and silver NPs were generated *in situ* inside the gels by heating at 100 °C for 1 h (without addition of a reducing agent).

Gold(I)-dodecanethiolate was dispersed into DGEBA/DA amphiphilic gels with the following procedure: 5 ml of a 5 mM solution of dodecanethiol (DDT) in THF were added slowly to 5 ml of a 1 mM solution of $HAuCl_4 \cdot 3H_2O$ in THF. This was followed by immersion of a squared slice of the physical gel (about 170 mg). The 5 : 1 molar ratio of DDT to $HAuCl_4 \cdot 3H_2O$ favors the formation of gold(I)-dodecanethiolate by the following reaction:[34]

$$HAuCl_4 + 3HSC_{12}H_{25} \rightarrow AuSC_{12}H_{25} + H_{25}C_{12}S\text{–}SC_{12}H_{25} + 4HCl$$

After about three hours, the gel was extracted from the reaction medium, rinsed three times with pure THF and dried slowly at room temperature (first in a closed vessel), to generate self-standing films.

Characterization techniques

Gel fractions and degrees of swelling of physical gels were determined gravimetrically from samples cut in squared pieces of approximately $1 \times 1 \times 0.2$ cm^3 (initial weight = W_0). After 24 h immersion in THF at room temperature, the supernatant was removed and slices blotted with filter paper and weighed in a stoppered vial (weight = W_s). Samples were then dried under vacuum to constant weight (weight = W_d). The gel fraction was defined by the ratio $W_d/W_0 \times 100$. The swelling degree was calculated as $[(W_s - W_d)/W_d] \times 100$.

Glass transition temperatures (T_g) were determined by differential scanning calorimetry (DSC, Perkin-Elmer Pyris 1) from scans performed at 10 °C min^{-1}. T_g was obtained from onset values of the change in specific heat during the heating scans.

Magnetic properties of gels infused with γ-Fe_2O_3@oleic acid NPs were measured in a commercial SQUID magnetometer in the 5–300 K temperature range under applied magnetic fields of up to 50 kOe.

Photoluminescence spectra in steady state were obtained with a Spex Fluoromax spectrofluorometer. The gel was supported on a glass holder placed at 45° with respect to the excitation beam. Measurements were performed using front face geometry at room temperature.

Transmission electron microscope (TEM) images were obtained using a Philips CM-12 microscope operated at an accelerating voltage of 100 kV. Ultrathin sections were cut on a Leica Ultracut R ultramicrotome equipped with a crio-ultramicrotomy EM-FCS camera.

HRTEM experiments were performed in a CM 200 Philips high-resolution transmission electron microscope equipped with an ultratwin objective lens at an acceleration voltage of 200 kV.

Scanning Electron Microscopy was performed employing a Philips 505 SEM equipment. A working distance of about 20–25 mm, an accelerating voltage of 15 kV, and a chamber pressure of 10^{-9} Torr were used.

Middle-infrared spectroscopy (Nicolet 6700 FTIR) was employed to characterize the nanocomposites. Measurements were carried out in the attenuated total reflectance mode (smart Orbit ATR accessory).

UV-vis spectra were recorded with an Agilent 8453 diode array spectrophotometer. Samples were placed in a 1 cm × 1 cm × 3 cm quartz cell and spectra recorded at room temperature.

A qualitative characterization of the uniformity of the dispersion of NPs in the gels was performed by observing the coloration of the cross-section of the samples by optical microscopy (Leica DMLB microscope).

Results and discussion

Characterization of the amphiphilic epoxy gels

Gels obtained by thermal annealing of DGEBA/dodecylamine (DA) and DGEBA/hexadecylamine (HA) linear polymers at 60 °C for 21 h were transparent materials with glass transition temperatures of 20 °C and 12 °C, respectively. The gel based on DGEBA/DA had a gel fraction of 80% and a 760% swelling degree in THF. Corresponding values for the gel based on DGEBA/HA were a gel fraction of 20% and a swelling degree in THF of 2950%. The higher gel fraction of DGEBA/DA with respect to DGEBA/HA arises from the fact that the tail-to-tail association of *n*-alkyl chains is more efficient the shorter the length of the alkyl chain.[29] This leads to a lower crosslink density and a higher swelling degree of the gel based on DGEBA/HA with respect to the one derived from DGEBA/DA. For practical purposes, gels based on DGEBA/DA are a more convenient choice than gels based on DGEBA/HA due to their high gel fractions and still significantly high swelling degrees. However, as will be reported in next section, the swelling degree determines the size of NPs that can be infused inside the physical gels.

The swelling degree of the DGEBA/DA gel in different solvents characterized by their solubility parameres[35] is shown in Fig. 2 (a similar behavior is expected for DGEBA/HA gels). The maximum swelling degree was observed for $CHCl_3$ with a solubility parameter, $\delta = 19$ $(MPa)^{1/2}$, indicating that this value is near the δ value of the amphiphilic gel. Swelling with both hydrophobic and hydrophilic solvents is very low with the exception of dimethylformamide (DMF) that produced a significantly high swelling degree (Fig. 2). Calculation of dispersion, polar and hydrogen bonding components of δ by group contributions[35] could not explain the different behavior found for this solvent. It is plausible that strong specific interactions between DMF and hydroxyl groups reported in the literature[36] could favor swelling of the gel.

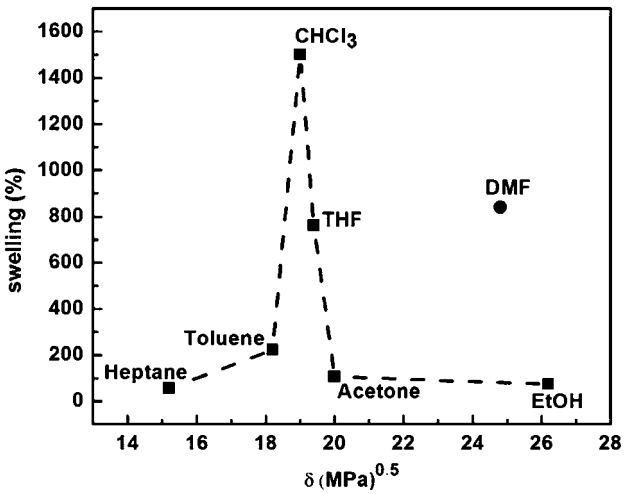

Fig. 2 Swelling degree of the DGEBA/DA gel in different solvents.

Infusion of pre-formed NPs into the amphiphilic epoxy gels

The introduction of NPs into the physical gels produced strongly colored nanocomposites. This helped to investigate the efficiency of the infusion process. The color homogeneity inside the sample cross-section (about 1 mm) was qualitatively determined by optical microscopy. For the different NPs and selected gels, results showed a uniform color inside the samples and a decrease of the coloration of the residual solutions. TEM micrographs (shown later in this section) confirmed that NPs were uniformly distributed inside the gels. Color of the samples was retained even after three exhaustive rinses in clear solvent, demonstrating the significant stability of the nanocomposites. The samples were finally dried in vacuum at room temperature.

Nanocomposites based on the infusion of γ-Fe_2O_3@oleic acid NPs will be discussed first. The infusion of these NPs into a DGEBA/DA gel was not possible due to large size of the NPs compared to the size of channels generated by swelling the gel in THF (the solvent used to disperse the NPs). The size of the core was about 3 nm but the actual size of the NPs was larger due to the contribution of the swollen oleic acid C18 chains that stabilize the NPs. In fact, an average hydrodynamic diameter of about 10 nm in heptane (obtained by dynamic light scattering) has been previously reported for these NPs.[31] However, the infusion process was successful when employing a DGEBA/HA gel. Increasing the length of the alkyl chain from C12 to C16, reduced the strength of tail-to-tail associations and led to gels exhibiting a significantly higher swelling degree in THF, as mentioned before. The generation of more open structures in the swollen gel facilitated the infusion of these NPs into the gel structure. This is a significant result because it implies that swollen DGEBA-*n*-alkylamine gels may be used to fractionate a population of NPs by sizes by using a convenient combination of the particular *n*-alkylamine and solvent. This could be used to eliminate undesired tails of very small particles generated in some techniques employed in the synthesis of NPs.

Materials obtained by exposure of the gels to the dispersion of γ-Fe_2O_3@oleic acid NPs in THF were strongly brown-colored as shown by a piece of the nanocomposite attracted by a magnet (Fig. 3a). A TEM micrograph and an HRTEM image (inset) showing the size, morphology and crystalline nature of iron oxide NPs used to obtain the magnetic nanocomposites are shown in Fig. 3b. The absence of large aggregates of NPs was supported by the magnetic behavior of γ-Fe_2O_3–DGEBA/HA ferrogels. The magnetization $M(T)$ as a function of temperature was measured for both zero-field-cooled (ZFC) and field-cooled

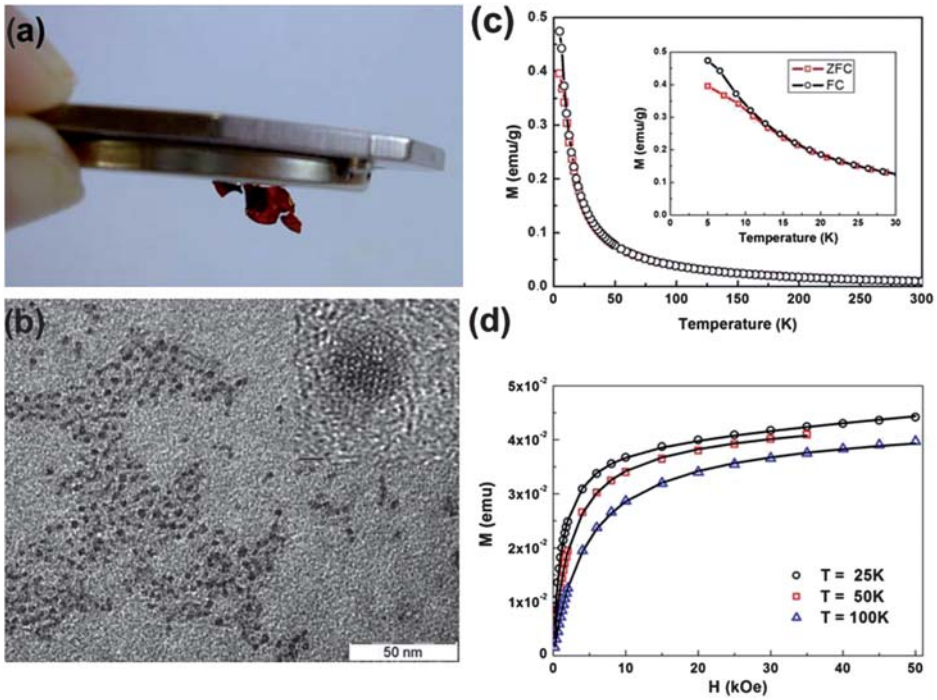

Fig. 3 (a) Photograph of a piece of a ferrogel based on DGEBA/HA, after exposure to a dispersion of γ-Fe_2O_3@oleic acid NPs in THF, attracted by a magnet; (b) TEM micrograph and an HRTEM image (inset) showing the size, morphology and crystalline nature of iron oxide NPs (bar in the inset = 1 nm); (c) Magnetization $M(T)$ of γ-Fe_2O_3–DGEBA/HA ferrogels as a function of temperature for both field-cooled (FC) and zero-field-cooled (ZFC) conditions (the inset is a magnification of the low T region); (d) $M(H)$ curves at different temperatures in the superparamagnetic regime, solid lines are the fitting curves with a Langevin function weighted by a log-normal size distribution.

(FC) conditions (Fig. 3c) under an applied magnetic field of 50 Oe. No maximum in the ZFC magnetization was observed down to 5 K indicating a very low blocking temperature (T_B). The FC magnetization curve increases with decreasing temperature and both ZFC and FC curves split at a $T_{irr} \approx 10$ K indicating the blocking of the largest particles. Therefore, the ferrogel can be characterized as a dispersion of weakly interacting superparamagnetic NPs.[37,38] This behavior is similar to that previously found for nanocomposites obtained with the same type of NPs dispersed in poly(vinylbutyral) matrices at loadings below 10 wt% (systems characterized by a uniform NPs dispersion).[39,40]

Magnetization curves as a function of applied magnetic field, $M(H)$, were measured at different temperatures (Fig. 3d). $M(H)$ curves in the superparamagnetic regime were fitted to an integral of a Langevin function weighted with a log-normal size distribution function. This fit was performed simultaneously for all temperatures (25 K, 50 K and 100 K). The fit yielded the value of magnetic moment corresponding to the average particle size $\mu =$ 170 (25) μ_B (μ_B: Bohr magneton) with a log-normal diameter dispersion of 0.3. Magnetite NPs of small diameters are usually found to present reduced saturation magnetization due to surface disorder.[41] Assuming a saturation value of magnetite NPs of ~40 emu g^{-1}, the magnetic moment ($\mu = 170\ \mu_B$) corresponds to a particle diameter of ~2.5 nm, close to the average value of the initial distribution of NPs (Fig. 3b). With this value of particle size and assuming a crystalline anisotropy of 5×10^5 erg cm^{-3}, a blocking temperature of the maximum of the size distribution of $T_B = 1$ K is obtained. Taking into account the log-normal size distribution, the maximum of the ZFC $M(T)$ curve would be located at $T_M = 1.6$ K, well below the lowest measured temperature.

The sample mass used in these magnetic measurements (of unloaded "dry" gel) was 11 mg. From the 5 K magnetization measured we estimate a 9% of magnetite mass as compared to the total sample mass. Considering the larger density of magnetite we estimate roughly a volumetric fraction of 2% magnetite in the gel.

In summary, magnetic response of the system supports the absence of large aggregates and the uniform dispersion of NPs in the sample.[39,40] As the efficiency of the tail-to-tail association of hexadecyl chains is relatively low, the structure of the physical gel must be composed of a set of associated alkyl chains producing the percolated structure of the physical gel and another set of unassociated hexadecyl chains pendant in the gel structure. These pendant chains can interact with the NPs stabilized with oleic acid chains preventing the presence of large aggregates inside the gel.

Au@DDT NPs were also incorporated inside DGEBA/DA physical gels by immersion of the polymers in the corresponding NPs dispersion in THF. The average size of the metallic core of the synthesized NPs was 2 nm.[19] Particles of this small size dispersed in THF could be efficiently infused into DGEBA/DA gels. Fig. 4a shows a photograph of the colored nanocomposite obtained after the infusion process in the swollen state. TEM images show the presence of aggregates of the individual NPs (Fig. 4b and c). As the tail-to-tail association of dodecyl chains is more efficient than the association of hexadecyl chains,[29] a low concentration of isolated pendant dodecyl chains in the gel

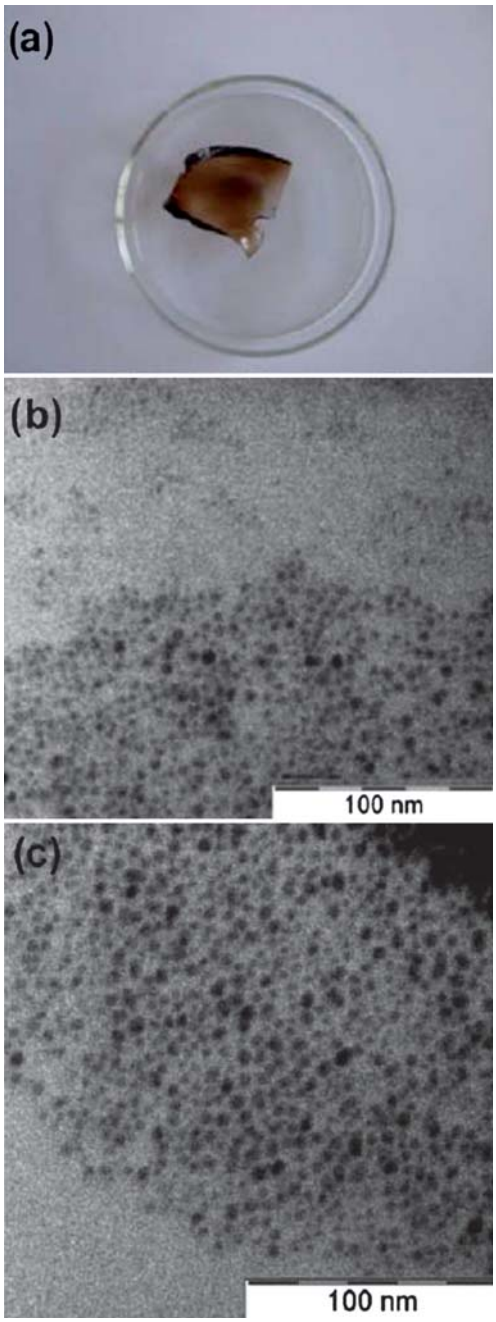

Fig. 4 (a) Photograph of a piece of DGEBA/DA amphiphilic gel infused with Au@DDT NPs in the swollen state, (b and c) TEM images from ultrathin cuts of Au@DDT NPs dispersed in a DGEBA/DA gel.

structure is expected. Pendant chains rather than associated chains are free to participate in the stabilization of dodecyl-coated NPs; their low concentration prevents an adequate stabilization and leads to a broad distribution of clusters of the infused NPs.

Fluorescent nanocomposites were obtained by immersion of a DGEBA/DA gel slice in an octadecene/THF dispersion of CdSe QDs (average size of 3 nm). Fig. 5a shows a HRTEM image of the initial CdSe dispersion in which crystalline planes of NPs can be observed. The emission spectrum of the semiconductor NPs at an excitation wavelength of 400 nm shows the presence of a characteristic and narrow emission band centered at 558 nm (Fig. 5b). TEM images of ultrathin cuts of the infiltrated gel showed NPs individually dispersed in the matrix as well as submicrometric aggregates in the gel structure (Fig. 5c). The emission spectrum of the nanocomposite, also obtained using an excitation wavelength of 400 nm, is shown in Fig. 5d. The band located at 558 nm is the characteristic fluorescent band of the selected QDs shown in Fig. 5b. The observed broadening could be attributed to the interactions of QDs with the matrix or to the small extent of aggregation observed in TEM images. It is known that fluorescence emission is quenched due to NPs aggregation.[42] As fluorescence of the nanocomposites was preserved and, at the same time, a large red-shifting of the emission band was not observed, the aggregation effect seems not to be so important in the infiltrated gel.

As a summary of this section, main properties of metal, iron oxide and semiconductor NPs were successfully transferred to the amphiphilic gels by simple infusion in dispersions of the preformed NPs. A convenient selection of the length of the alkyl chain in the gel and the specific solvent is necessary for an efficient infusion process.

In situ generation of NPs and gold thiolate inside the amphiphilic epoxy gels

Gold NPs were generated *in situ* inside DGEBA/DA gels. In a first step the gel was placed in contact with a THF solution of $HAuCl_4 \cdot 3H_2O$. This produced the simultaneous extraction of the sol fraction and the infusion of the gold complex inside the gel. FTIR spectra (not shown) revealed that the chemical composition of the sol was similar to one of the gel. UV-vis spectra of diluted solutions of the sol fraction and $HAuCl_4 \cdot 3H_2O$ in THF are shown in Fig. 6a. The sol exhibited two main absorption bands located at 238 nm and 277 nm while the gold(III) complex showed two main bands at 238 nm (overlapping with one of the bands of the sol), and at 327 nm. The tail of this last band in the visible region of the spectrum is responsible for the characteristic yellow color of gold(III) solutions. The solution that was initially placed in contact with the gel was yellow. The same color was rapidly observed for the gel due to the infusion of the gold(III) complex. However, after 72 h immersion both the gel and the solution became colorless. The UV-vis spectrum of the solution (Fig. 6b) shows the almost disappearance of the gold(III) band at 327 nm, that initially saturated the spectrum. This is explained by the reduction of Au^{3+} to Au^{1+} produced by the room-temperature reaction with OH groups present in the polymer chains.[43–49] The plasmon band of gold NPs was absent in this spectrum, evidencing that reduction to Au(0) did not occur at room temperature.

However, when the resulting gel was separated from the solution and heated for 1 h at 100 °C it turned to a dark red-colored material (Fig. 6c). This evidenced that Au^{1+} was reduced to Au(0) by OH groups present in the polymer gel without the addition of an external reducing agent.[43–49] A TEM image of the resulting nanocomposite shows that gold NPs exhibit a broad distribution of diameters ranging from 5 to 25 nm (Fig. 6d). NPs with this range of sizes could not have been infused into the DGEBA/DA gel. The *in situ* generation enabled to form relatively large NPs inside the amphiphilic gel avoiding the need of

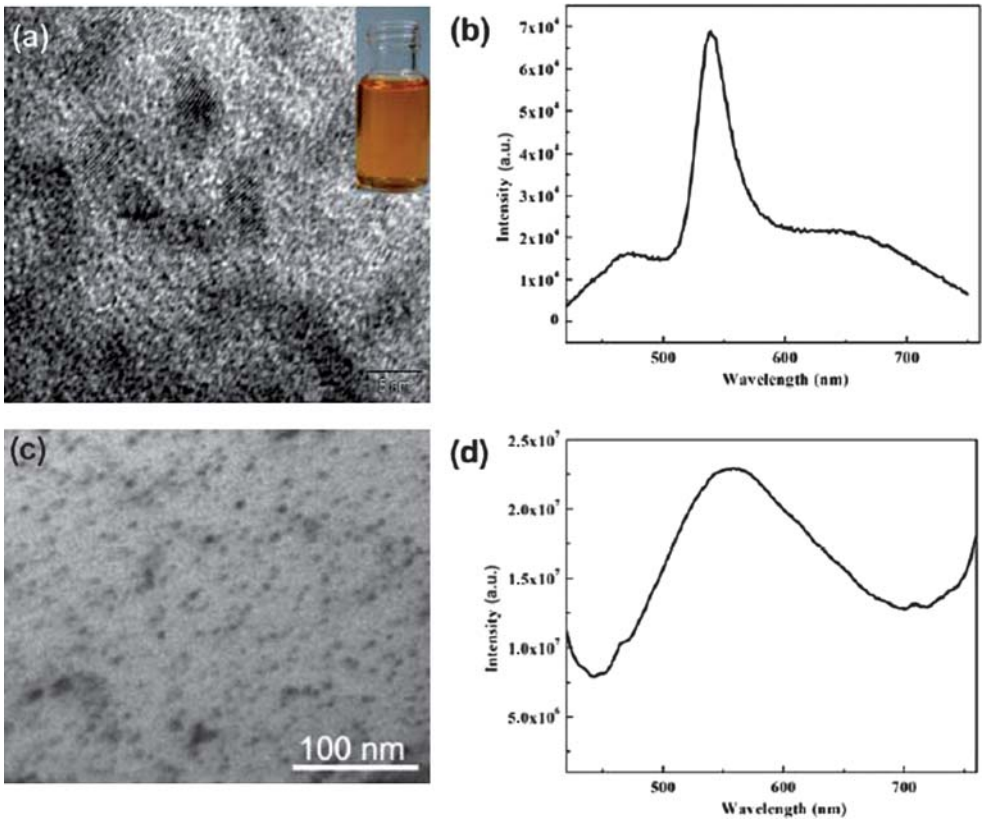

Fig. 5 (a) HRTEM image of the initial CdSe QDs (bar = 5 nm), the inset shows a photograph of the NPs dispersion in octadecene; (b) emission spectrum of the same dispersion at an excitation wavelength of 400 nm; (c) TEM image from an ultrathin cut of CdSe QDs dispersed in the DGEBA/DA gel; (d) emission spectrum of the nanocomposite based on CdSe QDs dispersed in the DGEBA/DA gel. The excitation wavelength was 400 nm.

using stabilizing organic groups (as those used for the pre-formed NPs). Another advantage of this process is related to the fact that the *in situ* generation of NPs in the presence of the amphiphilic polymer prevents the formation of large clusters in the resulting nanocomposite. Similar stabilizing effects for metallic NPs have been reported for amphiphilic poly(ethylene oxide)–poly(propylene oxide)–poly(ethylene oxide) block copolymers, explained by the adsorption of the hydrophobic block—poly (propylene oxide)—on the gold surface.[50–52] Based on these results it might be argued that in our system gold NPs are stabilized by the hydrophobic alkyl chains.

Although it is outside the scope of this study it is worth mentioning that there are several papers that analyzed the most important factors that promote the *in situ* generation of a nearly monodisperse distribution of NPs in a polymer matrix.[53–56] Modification of factors like reaction temperature, annealing time and temperature, concentration of precursors and chemical structure of the polymer host has been used to improve the size distribution of *in situ* generated NPs.

FTIR spectra of the neat DGEBA/DA gel, the Au^{1+}-modified gel (after 72 h immersion in the $HAuCl_4$ solution) and the gel with dispersed gold NPs (after 1 h at 100 °C) were recorded (Fig. 7). The three spectra showing the bands of the amphiphilic polymer were almost identical (Fig. 7a). However, some evidence of the changes produced by the presence of metallic gold or gold complexes was obtained. A small peak at 1150 cm^{-1}, present in the neat gel, assigned to the C–N stretch of the tertiary amine,[57] disappeared in samples containing gold salts or metallic gold. Additionally, a broad shoulder in the 2600 cm^{-1} region appeared in the spectra. A band in this region can be assigned to a trialkylammonium salt,[57] possibly originated by the reaction of the tertiary amine with $HAuCl_4$. Therefore, tertiary amine groups seem to be involved in the coordination of the gold complex with the polymer.

The reduction step may be schematically represented by the following equation (only two of the C bonds are indicated):[45]

$$HCOH + Au^{3+} \rightarrow C{=}O + 2H^{+} + Au^{1+}$$

Secondary alcohols are oxidized to ketones and the protons generated are trapped by tertiary amine groups (present in excess). A similar reaction takes into account the reduction of Au^{1+} to Au(0). It is usually difficult to find evidence of this mechanism in FTIR spectra due to the large excess of unmodified polymer. However, a very small band was found in the region comprised between 1660 cm^{-1} and 1670 cm^{-1} for the gel immersed in the $HAuCl_4$ solution for 72 h (Fig. 7b). This small band may be assigned to H-bonded ketone groups. A similar small band was present in the gel containing Au(0). In the region of OH stretching, the maximum observed for the neat gel at 3370 cm^{-1} was shifted to lower frequencies by the presence of Au^{1+} (3320 cm^{-1}) or Au(0) (3280 cm^{-1}), as observed in Fig. 7a. This indicates that OH groups of the amphiphilic gel are involved

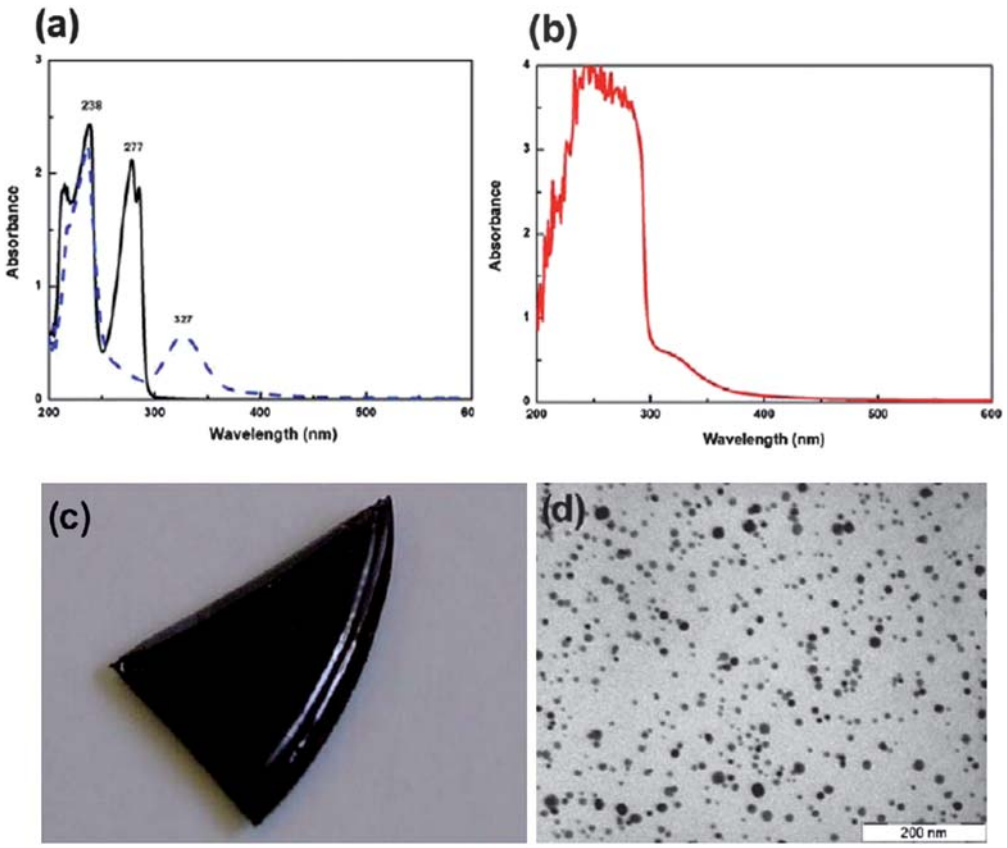

Fig. 6 (a) UV-visible spectra of diluted solutions of the sol extracted from the DGEBA/DA gel (full line) and $HAuCl_4 \cdot 3H_2O$ (dashed line) in THF; (b) UV-visible spectrum of the colorless solution after 72 h immersion; (c) photograph of the amphiphilic gel after the reduction step; (d) TEM image from an ultrathin cut showing gold NPs generated *in situ* in the DGEBA/DA gel.

in H-bonding, possibly with the ketone groups produced in the reaction.

The strength of the interactions of gold NPs with the amphiphilic polymer was evidenced by the significant increase of the glass transition temperature of the neat matrix ($T_g = 20$ °C) after the *in situ* generation of gold NPs ($T_g = 44$ °C).

A similar procedure of the one used for gold was performed starting from a solution of $AgNO_3$. After the final heating step, the transparent gel got a brown color characteristic of silver NPs. As in the case of gold, the amphiphilic polymer reduced Ag^+ to Ag(0) using its OH groups and without the need of adding a reducing agent. Fig. 8 shows a TEM image of the dispersion of silver NPs in the gel and a photograph of a thin piece of the amphiphilic gel after the reduction step (inset in Fig. 8). The dispersion of silver NPs was uniform and exhibited a broad distribution of sizes with an average in the order of 10 nm. FTIR spectra of the neat gel with silver NPs showed again the presence of a very small band at about 1665 cm^{-1}, assigned to H-bonded ketone groups. However, in this case the stretching band of the hydroxyl group experienced a smaller shift, from 3370 cm^{-1} to 3355 cm^{-1}, possibly due to the lower amount of ketone groups generated in reducing Ag^{1+} compared to Au^{3+}.

The interactions between the silver NPs and the amphiphilic gel were weaker than in the case of gold NPs. This was reflected by the small increase in the glass transition temperature, from 20 °C for the neat matrix to 28 °C for the nanocomposite containing silver NPs.

Gold(I)-alkanethiolate complexes exhibit highly ordered structures and a strong photoluminescence emission band in the visible region (λ close to 610 nm).[32] Besides, they can be converted into gold NPs stabilized by *n*-alkanethiolates by electron beam irradiation,[58] or by heating to an appropriate temperature.[59,60] However, they are highly insoluble powders, a fact that limits their use for practical applications. The feasibility of incorporating gold(I)-dodecanethiolate to a molten polystyrene matrix during processing has been reported,[60] although unavoidable clustering was observed in TEM images. Besides, at the processing temperatures partial decomposition of the gold(I)-dodecanethiolate might take place. Here, we investigated a different alternative consisting in generating the gold(I)-dodecanethiolate at room temperature in a THF-swollen DGEBA/DA amphiphilic gel immersed in excess solvent, following the procedure described in the Experimental section. Although gold(I)-dodecanethiolate precipitated slowly in the solution, a similar behavior occurred inside the amphiphilic gel. After separation of the gel and drying, self-standing films of uniform yellow color were obtained. Apart from the small band at 465 nm arising from the neat matrix, a strong red-emission band centered at 638 nm (for an excitation wavelength of 300 nm) was observed (Fig. 9a), revealing the successful generation of a luminescent nanocomposite.

It has been reported that thermal treatment of Au(I) *n*-alkanethiolates leads to a mixture of di-*n*-alkyl disulfide, di-*n*-alkyl

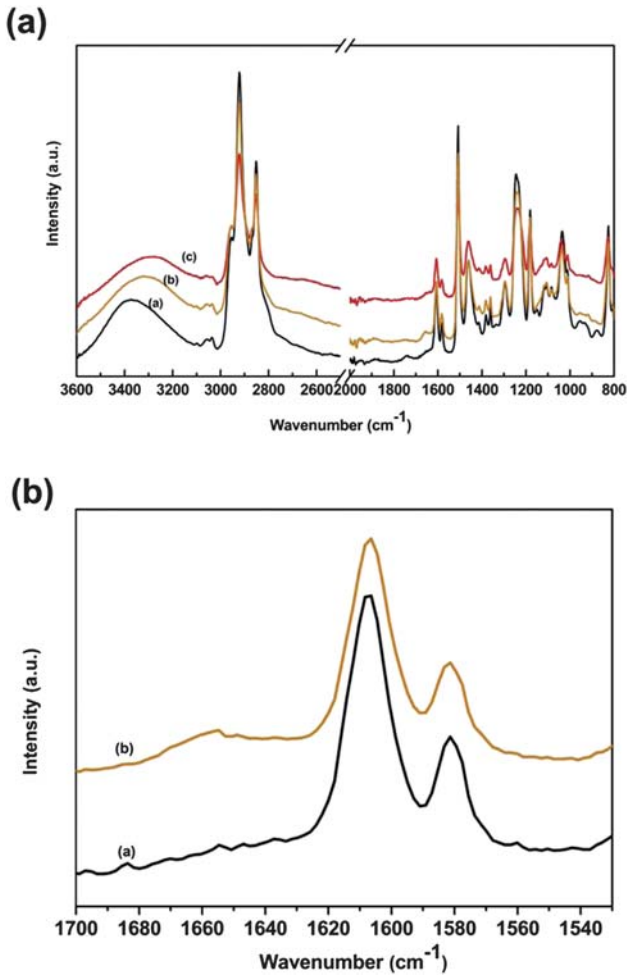

Fig. 7 (a) FTIR spectra of the neat DGEBA/DA gel (curve a), the gel obtained after 72 h immersion in the $HAuCl_4$ solution (curve b), and the gel after 1 h heating at 100 °C; (b) spectra of materials a and b expanded in the 1530 cm^{-1}–1700 cm^{-1} region.

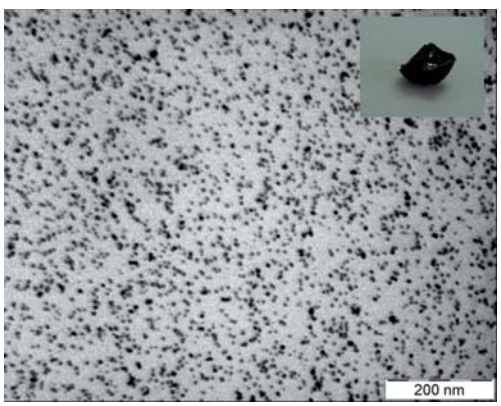

Fig. 8 TEM image of silver NPs generated *in situ* in the DGEBA/DA gel. The inset shows a photograph of a thin piece of the amphiphilic gel after the reduction step.

sulfide, and gold NPs stabilized by the *n*-alkanethiolates.[59] Fig. 9b and c show SEM images of the gel after 4 h of thermal treatment at 150 °C. Gold NPs of about 100 nm diameter uniformly distributed in the matrix can be clearly observed. The high dispersion level of NPs in the gel could be related to an efficient initial distribution of the thiolate in the matrix. Luminescence of the samples almost disappeared after heating for 4 h at 150 °C (data not shown), indicating complete conversion of the photoluminescent thiolate into gold NPs. However, preliminary results showed that samples treated for shorter times produced a partial conversion of Au(I) thiolate into Au(0) retaining the luminescence with a lower intensity. The co-existence of the luminescent gold thiolate and metallic gold in confined nanodomains could open the way to the development of multifunctional materials that share properties of both metal NPs and luminescent thiolates.

Conclusions

Amphiphilic physical gels containing hydrophilic and hydrophobic groups in their chemical structure were synthesized by the reaction of a diepoxy monomer based on diglycidyl ether of bisphenol A (DGEBA) with an *n*-alkylamine, followed by annealing the resulting linear polymers above their T_g. The chemical structure of the physical gel consists of a linear polar backbone with regularly spaced alkyl chains that are partially associated through tail-to-tail interactions. These gels exhibit a set of unique properties that make them suitable for the synthesis of a variety of advanced functional materials. Among the specific properties of interest are: (a) the high swelling capacity in organic solvents, *e.g.*, tetrahydrofuran (THF), dimethylformamide (DMF) or chloroform, employed to disperse inorganic NPs stabilized by organic ligands; (b) the presence of the polar group –CH(OH)–CH_2–N(R)–CH_2–CH(OH) suitable for the binding of some metallic ions, (c) the possibility to reduce gold and silver salts to the corresponding metals at convenient temperatures by oxidation of the OH groups, (d) the presence of non-associated alkyl chains that are useful to stabilize inorganic NPs, and (e) the significant influence of the length of the alkyl chain on the swelling degree of the physical gels that determines the range of sizes of pre-formed NPs that may be infused into the gels.

Pre-formed NPs could be successfully infused into the gels keeping their optical properties (*e.g.*, CdSe QDs) or magnetic behavior (*e.g.*, γ-Fe_2O_3@oleic acid NPs) in the resulting solid nanocomposite. The efficiency of the infusion process depends on the size of the NPs. Larger NPs require gels exhibiting high swelling degrees in the selected solvent. In turn, the swelling degree in a specific solvent can be controlled by selecting the length of the *n*-alkylamine. Increasing this length leads to an increase in the swelling degree due to the decrease in the fraction of tail-to-tail association of alkyl chains with a corresponding decrease in the crosslink density of the gel. This property might be useful to fractionate a population of NPs by sizes. Using a convenient combination of the particular *n*-alkylamine and solvent, the resulting gels may be used to extract the smallest NPs up to a particular size. This could be used to eliminate undesired tails of very small particles generated in some techniques employed in the synthesis of NPs.

The amphiphilic gels exhibited also a capacity to extract metallic ions from their solutions in THF, DMF or $CHCl_3$. Examples were provided using $HAuCl_4$ or $AgNO_3$ but salts of Co^{2+} or Cu^{2+} dissolved in DMF could be also efficiently infused

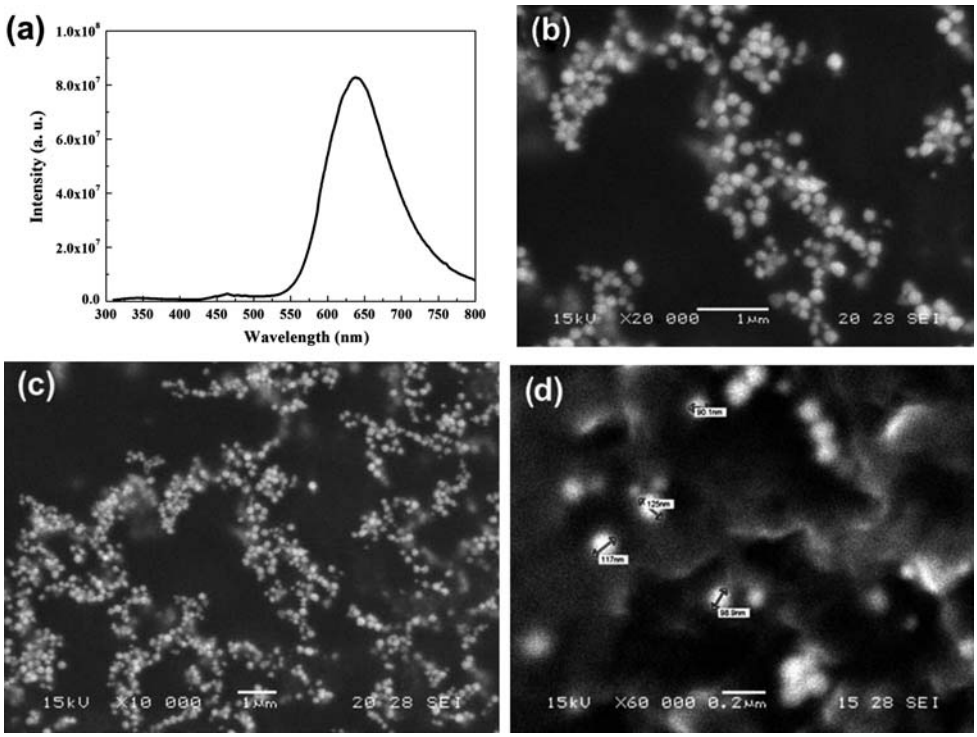

Fig. 9 (a) Luminescence spectrum of gold(I)-dodecanethiolate dispersed in the DGEBA/DA gel obtained with an excitation wavelength of 300 nm; (b–d) SEM images obtained from cross-sections of the same gel after 4 h of thermal treatment.

into the amphiphilic gels (unreported results). In the case of Au^{3+} and Ag^{1+} compounds, a reduction process to the corresponding metals was produced after a heating step. This led to a uniform distribution of metallic NPs inside the physical gel. The distribution of sizes was relatively broad in both cases with averages in the order of 10 nm. What is significant is the simplicity of the process: both the reducing capability and the stabilizing groups are provided by the amphiphilic gel. In the case of gold NPs a significant interaction with the amphiphilic polymer was proved by the significant increase of the matrix T_g (from 20 °C to 44 °C). Varying the concentration of metallic salt introduced into the amphiphilic gel and the reduction conditions can produce significant changes in the shape and size distribution of generated NPs (experiments in this direction are in progress).

Finally, the amphiphilic gel can be employed as a host for the *in situ* precipitation of an insoluble solid that becomes captured in a freestanding film. A uniform dispersion of gold(I)-dodecanethiolate inside a DGEBA/DA amphiphilic gel could be successfully obtained. The red light emission of the gold(I) complex was also observed in the amphiphilic gel. A variety of luminescent films might be obtained with this procedure.

Acknowledgements

We acknowledge the financial support of the National Research Council (CONICET, Argentina), the National Agency for the Promotion of Science and Technology (ANPCyT, Argentina), the University of Mar del Plata, the University of Buenos Aires (Argentina) and the Spanish Ministry of Science and Technology (MEC), project N° MAT2008-06503. A.L.S. acknowledges FPU grant from the MEC, Spain. The authors acknowledge Dr Horacio E. Troiani (CAB, CNEA) for HRTEM images. The financial support of the bilateral cooperation program "Luis Santaló" between Spain (CSIC) and Argentina (CONICET) is gratefully acknowledged.

References

1 G. Hodes, *Adv. Mater.*, 2007, **19**, 639.
2 A. L. Rogach, A. Eychmüller, S. G. Hickey and S. V. Kershaw, *Small*, 2007, **3**, 536.
3 R. Wilson, *Chem. Soc. Rev.*, 2008, **37**, 2028.
4 R. A. Sperling, P. Rivera Gil, F. Zhang, M. Zanella and W. J. Parak, *Chem. Soc. Rev.*, 2008, **37**, 1896.
5 C. Sun, J. S. H. Lee and M. Zhang, *Adv. Drug Delivery Rev.*, 2008, **60**, 1252.
6 R. Hao, R. Xing, Z. Xu, Y. Hou, S. Gao and S. Sun, *Adv. Mater.*, 2010, **22**, 2729.
7 Y. Xia, Y. Xiong, B. Lim and S. E. Skrabalak, *Angew. Chem., Int. Ed.*, 2009, **48**, 60.
8 M. Grzelczak, J. Pérez-Juste, P. Mulvaney and L. M. Liz-Marzán, *Chem. Soc. Rev.*, 2008, **37**, 1783.
9 J. P. Wilcoxon and B. L. Abrams, *Chem. Soc. Rev.*, 2006, **35**, 1162.
10 A. C. Balazs, T. Emrick and T. P. Russell, *Science*, 2006, **314**, 1107.
11 R. A. Vaia and J. F. Maguire, *Chem. Mater.*, 2007, **19**, 2736.
12 J. Jancar, J. F. Douglas, F. W. Starr, S. K. Kumar, P. Cassagnau, A. J. Lesser, S. S. Sternstein and M. J. Buehler, *Polymer*, 2010, **51**, 3321.
13 H. Zhang, J. Han and B. Yang, *Adv. Funct. Mater.*, 2010, **20**, 1533.
14 B. A. Rozenberg and R. Tenne, *Prog. Polym. Sci.*, 2008, **33**, 40.
15 Y. Ofir, B. Samanta and V. M. Rotello, *Chem. Soc. Rev.*, 2008, **37**, 1814.
16 R. J. J. Williams, B. A. Rozenberg and J. P. Pascault, *Adv. Polym. Sci.*, 1997, **128**, 95.
17 E. R. Soulé, J. Borrajo and R. J. J. Williams, *Macromolecules*, 2007, **40**, 8082.
18 I. A. Zucchi, M. J. Galante, R. J. J. Williams, E. Franchini, J. Galy and J. F. Gérard, *Macromolecules*, 2007, **40**, 1274.

19 I. A. Zucchi, C. E. Hoppe, M. J. Galante, R. J. J. Williams, M. A. López-Quintela, L. Matějka, M. Slouf and J. Pleštil, *Macromolecules*, 2008, **41**, 4895.
20 J. Greener, T. H. van der Loop, C. Paquet, G. Scholes and E. Kumacheva, *Langmuir*, 2009, **25**, 3173.
21 S. Dubinsky, A. Petukhova, I. Gourevich and E. Kumacheva, *Chem. Commun.*, 2010, **46**, 2578.
22 J. Choi, J. Harcup, A. F. Yee, Q. Zhu and R. M. Laine, *J. Am. Chem. Soc.*, 2001, **123**, 11420.
23 S. A. Pellice, D. P. Fasce and R. J. J. Williams, *J. Polym. Sci., Part B: Polym. Phys.*, 2003, **41**, 1451.
24 Y. L. Liu, G. P. Chang, K. Y. Hsu and F. C. Chang, *J. Polym. Sci., Part A: Polym. Chem.*, 2006, **44**, 3825.
25 I. E. dell'Erba, C. E. Hoppe and R. J. J. Williams, *Langmuir*, 2010, **26**, 2042.
26 C. Chang, J. Peng, L. Zhang and D. W. Pang, *J. Mater. Chem.*, 2009, **19**, 7771.
27 C. Feldgitscher, H. Peterlik, M. Puchberger and G. Kickelbick, *Chem. Mater.*, 2009, **21**, 695.
28 A. Salcher, M. S. Nikolic, S. Casado, M. Vélez, H. Weller and B. H. Juárez, *J. Mater. Chem.*, 2010, **20**, 1367.
29 J. Puig, I. A. Zucchi, C. E. Hoppe, C. J. Pérez, M. J. Galante, R. J. J. Williams and C. Rodríguez-Abreu, *Macromolecules*, 2009, **42**, 9344.
30 M. Brust, M. Walker, D. Bethell, D. J. Schiffrin and R. Whyman, *J. Chem. Soc., Chem. Commun.*, 1994, 801.
31 J. Vidal-Vidal, J. Rivas and M. A. López-Quintela, *Colloids Surf., A*, 2006, **288**, 44.
32 C. B. Murray, D. J. Norris and M. G. Bawendi, *J. Am. Chem. Soc.*, 1993, **115**, 8706.
33 E. M. Boatman, G. C. Linsenky and K. J. Nordell, *J. Chem. Educ.*, 2005, **82**, 1697.
34 S. H. Cha, J. U. Kim, K. H. Kim and J. C. Lee, *Chem. Mater.*, 2007, **19**, 6297.
35 A. F. M. Barton, *Handbook of Solubility Parameters and Other Cohesion Parameters*, CRC Press, Boca Raton, FL, 1983.
36 A. M. E. Raj, L. B. Resmia, V. B. Jothyb, M. Jayachandranc and C. Sanjeevirajad, *Fluid Phase Equilib.*, 2009, **281**, 78.
37 J. L. Dormann, D. Fiorani and E. Tronc, *Adv. Chem. Phys.*, 1997, **98**, 283.
38 G. A. Held, G. Grinstein, H. Doyle, S. Sun and C. B. Murray, *Phys. Rev. B: Condens. Matter Mater. Phys.*, 2001, **64**, 012408.
39 C. E. Hoppe, F. Rivadulla, J. Vidal-Vidal, M. A. López-Quintela and J. Rivas, *J. Nanosci. Nanotechnol.*, 2008, **8**, 2883.
40 C. E. Hoppe, F. Rivadulla, M. A. López-Quintela, M. C. Buján, J. Rivas, D. Serantes and D. Baldomir, *J. Phys. Chem. C*, 2008, **112**, 13099.
41 J. M. Vargas, E. Lima, Jr, R. D. Zysler, J. G. Santos Duque, E. De Biasi and M. Knobel, *Eur. Phys. J. B*, 2008, **64**, 211.
42 M. V. Artemyev, U. Woggon, H. Jaschinski, L. I. Gurinovich and S. V. Gaponenko, *J. Phys. Chem. B*, 2000, **104**, 11617.
43 H. Hirai, Y. Nakao and N. Toshima, *J. Macromol. Sci., Part A: Pure Appl. Chem.*, 1979, **13**, 727.
44 S. A. Yeung, R. Hobson, S. Biggs and F. Grieser, *J. Chem. Soc., Chem. Commun.*, 1993, 378.
45 Z. Y. Huang, G. Mills and B. Hajek, *J. Phys. Chem.*, 1993, **97**, 11542.
46 L. M. Liz-Marzán and I. Lado-Tourino, *Langmuir*, 1996, **12**, 3585.
47 Y. Sun and Y. Xia, *Science*, 2002, **298**, 2176.
48 B. Wiley, T. Herricks, Y. Sun and Y. Xia, *Nano Lett.*, 2004, **4**, 1733.
49 B. Wiley, Y. Sun, B. Mayers and Y. Xia, *Chem.–Eur. J.*, 2005, **11**, 454.
50 T. Sakai and P. Alexandridis, *Langmuir*, 2004, **20**, 8426.
51 T. Sakai and P. Alexandridis, *J. Phys. Chem. B*, 2005, **109**, 7766.
52 T. Sakai and P. Alexandridis, *Langmuir*, 2005, **21**, 8019.
53 S. Porel, S. Singh, S. S. Harsha, D. N. Rao and T. P. Radhakrishnan, *Chem. Mater.*, 2005, **17**, 9.
54 G. Carotenuto, G. La Peruta and L. Nicolais, *Sens. Actuators, B*, 2006, **114**, 1092.
55 Z. Zhanga and M. Han, *J. Mater. Chem.*, 2003, **13**, 641.
56 C. Feldgitscher, H. Peterlik, M. Puchberger and G. Kickelbick, *Chem. Mater.*, 2009, **21**, 695.
57 B. Smith, *Infrared Spectral Interpretation, a Systematic Approach*, CRC Press, Boca Raton, FL, 1999.
58 J. U. Kim, S. H. Cha, K. Shin, J. Y. Jho and J. C. Lee, *J. Am. Chem. Soc.*, 2005, **127**, 9962.
59 S. H. Cha, K. H. Kim, J. U. Kim, W. K. Lee and J. C. Lee, *J. Phys. Chem. C*, 2008, **112**, 13862.
60 A. S. Susha, M. Ringler, A. Ohlinger, M. Paderi, N. LiPira, G. Carotenuto, A. L. Rogach and J. Feldmann, *Chem. Mater.*, 2008, **20**, 6169.